INTERNATIONAL JOURNAL FOR NUMERICAL METHODS IN FLUIDS
Int. J. Numer. Meth. Fluids 2011; **67**:700–712
Published online 5 August 2010 in Wiley Online Library (wileyonlinelibrary.com). DOI: 10.1002/fld.2384

Shear-improved Smagorinsky modeling of turbulent channel flow using generalized Lattice Boltzmann equation

Saeed Jafari and Mohammad Rahnama*, †

Mechanical Engineering Department, Shahid Bahonar University of Kerman, Kerman, Iran

SUMMARY

Generalized Lattice Boltzmann equation (GLBE) was used for computation of turbulent channel flow for which large eddy simulation (LES) was employed as a turbulence model. The subgrid-scale turbulence effects were simulated through a shear-improved Smagorinsky model (SISM), which is capable of predicting turbulent near wall region accurately without any wall function. Computations were done for a relatively coarse grid with shear Reynolds number of 180 in a parallelized code. Good numerical stability was observed for this computational framework. The results of mean velocity distribution across the channel showed good correspondence with direct numerical simulation (DNS) data. Negligible discrepancies were observed between the present computations and those reported from DNS for the computed turbulent statistics. Three-dimensional instantaneous vorticity contours showed complex vortical structures that appeared in such flow geometries. It was concluded that such a framework is capable of predicting accurate results for turbulent channel flow without adding significant complications and the computational cost to the standard Smagorinsky model. As this modeling was entirely local in space it was therefore adapted for parallelization. Copyright © 2010 John Wiley & Sons, Ltd.

Received 28 October 2009; Revised 15 March 2010; Accepted 1 June 2010

KEY WORDS: Lattice Boltzmann method; large eddy simulation; turbulent flow; Smagorinsky model; channel flow

INTRODUCTION

Lattice Boltzmann method (LBM) has attracted much attention as a promising alternative for simulation of fluid flows with complex physics in the past two decades [1–4]. LBM is a method based on the solution of Boltzmann equation on a lattice with discrete velocity field. It was shown that basic conservation equations of fluid flow (Navier–Stokes equations) can be obtained from the Boltzmann equation [5]. The solution of the detailed balance provides a velocity distribution function from which macroscopic fluid properties, such as density, velocity and pressure are computed. Using LBM for computing fluid flow problems has some advantages as compared with CFD; among them are lack of a nonlinear convective term in the Lattice Boltzmann equation and simple pressure computation using an equation of state [2]. Moreover, the streaming-and-collision computational procedure of LBM, which is a local operation in its computational procedure, makes it an excellent candidate for parallel computing [6, 7].

Turbulent flow occurs in many engineering applications. Its computation suffers from two main restrictions: inability to solve the wide range of scales especially at high Reynolds numbers and accurate modeling of eddies in unresolved subgrid scale. While direct numerical simulation (DNS)

*Correspondence to: Mohammad Rahnama, Mechanical Engineering Department, Shahid Bahonar University of Kerman, Kerman, Iran.
†E-mail: mrah1338@gmail.com

of turbulent flow is the most accurate method for turbulent flow computations, its high computational cost prevents it from being applied to many fluid flow situations. Large eddy simulation (LES) has been considered as an alternative to DNS due to its ability to compute large scales directly while modeling universal small scales with an appropriate subgrid scale (SGS) modeling. In fact, LES is an affordable and accurate substitution for DNS of turbulent flows. An important advantage of LES is its ability to approach DNS with improved computational facilities and/or more accurate SGS modeling. The remarkable progress in the development of LES for turbulent flows and its application has been discussed in Reference [8].

Discrete kinetic theory, and in particular the LBM, has recently been used to *a priori*-derived turbulence models based on mean field approximation [9]. LES computations can be done using LBM, for which different configurations have been considered recently [6, 7, 10–12]. The simplest SGS model used in LES is the Smagorinsky model. Fernandino *et al.* [10] performed an LES of free surface duct flow using LBM in which Smagorinsky subgrid scale (SGS) model was used. Their results showed that the simple SGS model could be used as a possible tool for the simulation of free surface duct flow. In another study, Lammers *et al.* [11] showed that a high-resolution DNS of plane-channel turbulent flow at $Re_\tau = 180$ using LBM is capable of producing statistics of the same quality as pseudo-spectral methods, at resolutions comparable to, and in fact better than those of the pseudo-spectral runs. Spasov *et al.* [12] compared DNS of turbulent channel flow computed through LBM with entropic Lattice Boltzmann method (ELBM). They concluded that LBM can be used as a tool to simulate turbulent flows and ELBM scheme can be utilized to achieve accurate results with reasonably low grid resolution.

An important parameter in LBM computation is the relaxation time which appears in modeling of the collision term. A single relaxation time (SRT) is used in BGK LBM [13], which has been used for a wide range of fluid flow problem because of its simplicity [5–7, 10, 11]. Numerical instability of SRT along with the lack of a proper mechanism for dissipation of small-scale unphysical oscillations arising from the kinetic model were the main reasons for shifting toward multiple relaxation time (MRT) LBM. MRT LBM which is sometimes called generalized Lattice Boltzmann equation (GLBE), shows a significant improvement in the numerical stability as compared with SRT LBM [14–21], which in turn, makes it suitable for the simulation of turbulent flows.

Premnath *et al.* [19] presented a framework for LES using GLBE with a forcing term, for wall-bounded flows in which, the forcing term shows the effect of external forces, such as constant body forces representing pressure gradient in a periodic domain. They emphasized the numerical stability of their method even on a coarse grid and its ability to be used in a variable-resolution multiblock approach. Assessment of their method was done for two geometries: fully developed channel flow and shear-driven flow in a cubical cavity. Channel flow studies were reported for a Reynolds number of 183.6 based on friction velocity and channel half-width. Their results showed good agreement with DNS and experimental data. Moreover, implementation of GLBE showed excellent parallel scalability on a large parallel cluster with over a thousand processors [19].

GLBE was also used for the simulation of turbulent duct flow [20] in which SGS stresses were modeled through Smagorinsky eddy viscosity model, and channel flow [21] with incorporation of dynamic procedure for LES. The effectiveness of GLBE was shown in both research works through good results obtained using this method; it seems that GLBE is a firm framework for further turbulent flow investigations.

Recently, Lèvêque *et al.* [22] proposed a shear-improved Smagorinsky model (SISM) in which the Smagorinsky eddy viscosity is computed from the difference between the magnitude of mean shear and that of the instantaneous resolved strain-rate tensor. Their results for LES of channel flow showed excellent agreement with DNS and dynamic Smagorinsky model. Moreover, no wall function is needed for this model and its computational cost was reported to be lower than DNS. This model was employed for the present computations of channel flow.

The present work is focused on the application of SISM [22] in LES computation of turbulent flow which is carried out through GLBE. A benchmark problem of wall-generated turbulent flow, i.e. a fully developed turbulent channel flow at shear or friction Reynolds number of 180 was considered as a test case for evaluating the abovementioned computational procedure. There is an extensive

DOI: 10.1002/fld

amount of experimental and DNS data available for the assessment and comparison of the detailed structure of turbulent statistics for this geometry [19, 23]. It is worth mentioning that all the previous applications of SISM were reported using computational methods based on CFD. This model which is capable of revealing near-wall flow characteristics without any wall-damping function has not been used in MRT LBM before. Computational results showed that this model is also applicable to a coarse grid with good numerical stability and possibility of doing parallel processing.

GENERALIZED LATTICE BOLTZMANN METHOD WITH FORCING TERM

LBM is based on the computation of a distribution function of particles as they move and collide on a lattice grid. The collision process considers their relaxation to their local equilibrium values, and the streaming process describes their movement along the characteristic directions given by a discrete particle velocity space represented by a lattice [1–4]. GLBE, computes the collisions in moment space, while the streaming process is performed in the usual particle velocity space [14, 15]. This method is based on multiple relaxation times (MRT) which enhances its numerical stability. GLBE with forcing term [19–21] which incorporates an additional forcing term, represents the effect of external forces as a second-order accurate time discretization in moment space. GLBE with forcing term can be written in the following form [19]:

$$\mathbf{f}(\vec{x}+\vec{e}\delta t, t+\delta t)=\mathbf{f}(\vec{x},t)-M^{-1}.\hat{S}.[\mathbf{m}-\mathbf{m}^{\mathrm{eq}}(\rho,\vec{u})](\vec{x},t)+M^{-1}.\left(I-\frac{1}{2}\hat{S}\right).\mathbf{S}(\vec{x},t) \tag{1}$$

Here, $\mathbf{f}$ is the velocity distribution function and ρ and $\vec{u}$ are the macroscopic density and velocity, respectively. The bold face symbols, i.e. $\mathbf{f}$, $\mathbf{m}$ and $\mathbf{S}$ stand for 19-component vectors where 19 is the number of discrete velocities. Therefore, $\mathbf{f}$ in Equation (1) is the 19-component vector of the discrete distribution functions, $\mathbf{m}$ and $\mathbf{m}^{\mathrm{eq}}$ are 19-component vectors of moments and their equilibria, $\mathbf{S}$ is the 19-component vector of the source terms in moment space, $\mathbf{M}$ is the transformation matrix and $\hat{S}$ is the diagonal matrix of relaxation rates.

The collision and source terms are expressed in moment space in this equation. Here, M is an orthogonal transformation matrix with 19×19 elements, mapping the velocity distribution vector $\mathbf{f}$ to the moment vector $\mathbf{m}$ in the moment space. The collision matrix in velocity space, Λ, is related to $\hat{S}$ in Equation (1) through the relation $\hat{S}=M\Lambda M^{-1}$ such that $\hat{S}$ is a diagonal matrix. The elements of M are obtained in a suitable orthogonal basis as combinations of monomials of the Cartesian components of the particle velocity $\vec{e}_\alpha$ through the standard Gram–Schmidt procedure, which are provided by d'Humières *et al.* [15]. Components of moments, $\mathbf{m}$, their equilibria, $\mathbf{m}^{\mathrm{eq}}$, and the source term, $\mathbf{S}$, are mentioned in references [19–21].

The last term in Equation (1) shows the effect of an external force field on the evolution of the distribution function. While different external force fields may exist such as gravity, Lorentz or Coriolis forces, pressure gradient in a periodic domain may also be considered as an external force field, a technique which is used in the present computation.

Figure 1 shows the three-dimensional, 19 particle-velocity-lattice (D3Q19) model which has been widely and successfully used for the simulation of three-dimensional flows. In this model, the particle velocity $\vec{e}_\alpha$ may be written as:

$$\begin{aligned}
&\vec{e}_0=(0,0,0), \quad \alpha=0\\
&\vec{e}_\alpha=(\pm1,0,0)c,(0,\pm1,0)c,(0,0,\pm1)c, \quad \alpha=1,\ldots,6\\
&\vec{e}_\alpha=(\pm1,\pm1,0)c,(\pm1,0,\pm1)c,(0,\pm1,\pm1)c, \quad \alpha=7,\ldots,18
\end{aligned} \tag{2}$$

Here $c=\delta x/\delta t$, where δx and δt are the lattice spacing and the time increment, respectively and are assumed to be unity. The macroscopic density and momentum on each lattice node are calculated

DOI: 10.1002/fld

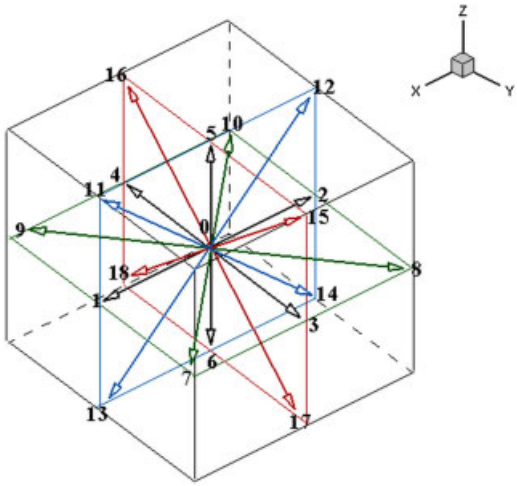

Figure 1. D3Q19 lattice model.

using the following equations:

$$\rho = \sum_{\alpha=0}^{18} f_\alpha \tag{3}$$

$$\vec{j} = \rho\vec{u} = \sum_{\alpha=1}^{18} \vec{e}_\alpha f_\alpha + \frac{1}{2}\vec{F}\,\delta t \tag{4}$$

Here $\vec{F}$ is an external force. Pressure can be obtained from an equation of state which is similar to that of an ideal gas, i.e. $P = \rho c_s^2$. The speed of sound, c_s, in D3Q19 model is written as $c_s = c/\sqrt{3}$. The grid-filtered weakly compressible Navier–Stokes equations with an external force can be obtained through a multiscale analysis based on the Chapman–Enskog expansion [24, 25] applied to the GLBE with relaxation time scales augmented by an eddy viscosity [21]. It should be noted that all the quantities used in Equation (1) are filtered quantities used in LES.

The diagonal matrix $\hat{S}$ of relaxation rates $\{s_i\}$ is given as $\hat{S} = \mathrm{diag}(s_0, s_1, \ldots, s_{18})$, where some of the relaxation times s_α in this diagonal matrix, i.e. those corresponding to hydrodynamic modes can be related to the transport coefficients and modulated by eddy viscosity due to SGS model [15, 18, 19] as: $s_1^{-1} = 0.5(9\zeta + 1)$, where ζ is the molecular bulk viscosity, $s_9 = s_{11} = s_{13} = s_{14} = s_{15} = s_\nu$, with $s_\nu^{-1} = 3\nu + 0.5 = 3(\nu_0 + \nu_t) + 0.5$. Here, ν_0 and ν_t are kinematic and eddy viscosities, respectively. Other relaxation rates are usually indicated through the von Neumann stability analysis of the linearized GLBE [15] as $s_1 = 1.19$, $s_2 = s_{10} = s_{12} = 1.4$, $s_4 = s_6 = s_8 = 1.4$ and $s_{16} = s_{17} = s_{18} = 1.98$.

The source terms in moment space are functions of external force, $\vec{F}$, and velocity field, $\vec{u}$. Their relations are presented in References [19–21]. The components of the strain rate tensor used in SGS turbulence model at the grid-filter level can be written explicitly in terms of non-equilibrium moments augmented by moment projections of source terms without the need to apply finite differencing of the velocity field, as [19]:

$$S_{xx} \approx -\frac{1}{38\rho}[s_1 h_1^{\mathrm{neq}} + 19 s_9 h_9^{\mathrm{neq}}] \tag{5}$$

$$S_{yy} \approx -\frac{1}{76\rho}[2s_1 h_1^{\mathrm{neq}} - 19(s_9 h_9^{\mathrm{neq}} - 3s_{11} h_{11}^{\mathrm{neq}})] \tag{6}$$

$$S_{zz} \approx -\frac{1}{76\rho}[2s_1 h_1^{\mathrm{neq}} - 19(s_9 h_9^{\mathrm{neq}} + 3s_{11} h_{11}^{\mathrm{neq}})] \tag{7}$$

DOI: 10.1002/fld

$$S_{xy} \approx -\frac{3}{2\rho} s_{13} h_{13}^{\text{neq}} \tag{8}$$

$$S_{yz} \approx -\frac{3}{2\rho} s_{14} h_{14}^{\text{neq}} \tag{9}$$

$$S_{xz} \approx -\frac{3}{2\rho} s_{15} h_{15}^{\text{neq}} \tag{10}$$

$$h_{\alpha}^{\text{neq}} = m_{\alpha} - m_{\alpha}^{\text{eq}} + \tfrac{1}{2} S_{\alpha} \tag{11}$$

The magnitude of the strain rate tensor,$|S|$, in turbulence models can be obtained from the above equations as $|S| = \sqrt{2S_{ij}S_{ij}} = \sqrt{2[S_{xx}^2 + S_{yy}^2 + S_{zz}^2 + 2(S_{xy}^2 + S_{yz}^2 + S_{xz}^2)]}$. The driving force in the present channel flow computation is pressure gradient which is related to τ_w and therefore shear velocity through: $\vec{F} = -\frac{\mathrm{d}p}{\mathrm{d}x}\vec{x} = \frac{\tau_w}{H}\vec{x} = \frac{\rho u_\tau^2}{H}\vec{x}$.

SHEAR-IMPROVED SMAGORINSKY MODEL (SISM)

The SISM which was proposed by Lèvêque *et al.* [22] is a model for computing SGS stresses used in LES computations of the present work. It is based on the fact that SGS eddy viscosity should encompass two types of interactions: (i) between the mean velocity gradient and the resolved fluctuating velocities (the rapid part of the SGS fluctuations [26]) and (ii) among the resolved fluctuating velocities themselves (the slow part of the SGS fluctuations). The rapid part is related to the large-scale distortion, while the slow part is associated with the Kolmogorov's energy cascade. These developments end up with an SISM [22] for the SGS eddy viscosity, in which it appears that the shear should be subtracted from the magnitude of the resolved rate-of-strain tensor. This improvement accounts for the large-scale distortion in regions of strong shear (e.g. near a solid boundary) and, at the same time, allows us to recover the standard Smagorinsky model in regions of locally homogeneous and isotropic turbulence (at grid scale). The SISM does not call for any adjustable parameter nor *ad hoc* damping function; it does not use any kind of dynamic adjustment either. Results concerning a plane-channel flow [22] and a backward-facing step flow [27] have shown good predictive capacity of this model, essentially equivalent to the dynamic Smagorinsky model [28], but with a computational cost and manageability comparable to the original Smagorinsky model. It should be mentioned that the computational cost would be increased if temporal averaging is added to the spatial averaging, a situation which does not occur in the present study. In such cases, the aforementioned advantage may become questionable. SISM Eddy viscosity is obtained by subtracting the magnitude of the shear from the instantaneous resolved rate of strain:

$$v_T^{\text{SISM}}(x,t) = (C_S\Delta)^2(|S_\Delta(x,t)| - S(x,t)) \tag{12}$$

Here, $S(x,t)$ denotes the shear at position x and time t, $|S_\Delta(x,t)|$ shows the magnitude of instantaneous resolved rate of strain at position x and time t, C_S is the Smagorinsky constant for homogeneous and isotropic turbulence ($C_S \approx 0.18$) and $\Delta = (\Delta x \Delta y \Delta z)^{1/3}$ is the width of the grid filter and, Δx, Δy and Δz are the local grid spacing in x, y and z directions, respectively. It is assumed that the flow is resolved well enough in the direction of the shear, so that

$$S(x,t) \approx |\langle S_\Delta(x,t)\rangle| \tag{13}$$

In flow regions where the fluctuating part of the rate of strain is much larger than the shear, i.e. $|S'_\Delta| \geqslant S$, width of the grid filter $\Delta \leqslant L_S$ by assuming that $|S'_\Delta| = u'/\Delta$. In that case, turbulence can be considered as homogenous and isotropic at a scale comparable to Δ. The SIMS then reduces to the original Smagorinsky model, which is known to perform reasonably well. In flow regions where $|S'_\Delta| \leqslant S$, width of the grid filter $\Delta \geqslant L_S$ and therefore shear effects are significant at scales

DOI: 10.1002/fld

comparable to Δ. In that case, the SISM yields an SGS energy flux of order $\Delta^2 S(|S'_\Delta|^2)$, which is fully consistent with the SGS energy budget that can be derived from the Navier–Stokes equations in the case of a locally homogenous flow [22].

In the present work, spatial averaging over x and y directions (homogenous directions in channel flow) is used to compute $|\langle S_\Delta(x,t)\rangle|$ and Equations (5)–(11) are employed to obtain the magnitude of the instantaneous resolved rate of strain. Therefore, Equation (12) can be written in the following form:

$$\nu_T^{\mathrm{SISM}}(x,t)=(C_S\Delta)^2(|S|-|\langle S_\Delta(x,t)\rangle|) \tag{14}$$

ν_T^{SISM} obtained from above equation is used as an eddy viscosity, ν_t, in expression for relaxation rate as: $s_\nu^{-1}=3\nu+0.5=3(\nu_0+\nu_t)+0.5$.

COMPUTATIONAL DETAILS

The geometry of a fully developed channel flow is shown in Figure 2. The linear dimensions of the domain are $6H$ and $3H$ in the streamwise and spanwise directions respectively, where H is the channel half-height. The flow is assumed to be homogeneous in both spanwise and streamwise directions, while a mean pressure gradient exists in the streamwise direction. Reynolds number based on the shear velocity and channel half-width is considered as $Re_\tau=u_\tau H/\nu=180$ for which previous DNS data exists [23].

Boundary conditions used in the present computations are: (i) periodic boundary condition [1] in the streamwise and spanwise directions due to the existence of fully developed flow in streamwise and homogeneity in spanwise, (ii) half way bounce-back boundary condition [29], which is second order in space [29], for the bottom solid wall of the channel and (iii) free slip boundary condition [1] at the top boundary.

A uniform grid was used for the present computations. The number of nodes in streamwise, spanwise and cross-stream directions was selected as 240, 120 and 40, respectively, which corresponds to a mesh with a resolution of 4.5 wall units in each direction. Although the total number of 11 52 000 grid points corresponds to a coarse grid distribution, the accuracy of the computational results has not been affected significantly as will be discussed in the results section. Recently, it was shown [12] that for $Re_\tau=u_\tau H/\nu=180$ the channel half-width has to be $H\geqslant 120$ if the simulation is to be considered a DNS which clearly justify low computational grid points of GLBE as compared with DNS. The computer code was parallelized with MPICH2 bindings and the domain was divided in slices along the streamwise direction. The computational time for one lattice time step was around 0.55 s while two processors were used.

The initial mean velocity is specified to satisfy the 1/7 power law, while the initial perturbations satisfy a divergence-free velocity field [19–21]. It is worth mentioning that a suitable initial

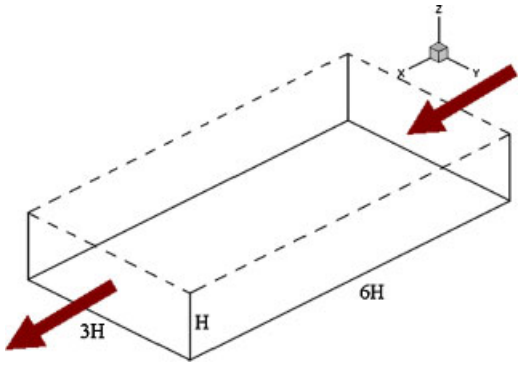

Figure 2. Simulation geometry.

DOI: 10.1002/fld

condition can significantly decrease the number of iterations needed for the convergence of the solution to a statistically steady-state condition.

RESULTS

Fully developed turbulent channel flow is a simple flow geometry which may be considered as a benchmark problem in assessing various computational procedure and turbulent models. This flow geometry has been studied by various authors, e.g. DNS and LES based on Navier–Stokes equations [22, 23], LES and DNS based on SRT-LBE [11] and MRT-LBE [19–21]. Recently, an SISM of LES computation of channel flow [22] showed its accuracy as compared with dynamic LES models with lower computational cost. The results were presented with the aim of evaluation of SISM of LES based on GLBE computations for a relatively coarse grid. The flow Reynolds number considered in the present study was selected as $Re_\tau = 180$ based on shear velocity and half channel width.

The first computational result presented here is the mean velocity profile normalized by the shear velocity u_τ versus distance from the wall in terms of wall units, i.e. $z^+ = z/\delta$ where δ is the viscous length scale, see Figure 3. The DNS data of Kim *et al.* [23] was presented in this figure for comparison. It is observed that the mean velocity profile computed from GLBE corresponds to DNS data relatively well, especially for the near wall region, although a finer grid was used by Kim *et al.* [23] than the one used in the present computations. The small differences observed in the regions far from the wall, may be due to the slip boundary condition used in the present computation for a half channel as compared with a no-slip boundary condition for a full channel. The reason for using half channel was the limited computational hardware available for the present computations.

The linear velocity profile in viscous sublayer and the logarithmic variations in the inertial sublayer of channel flow are shown in Figure 4 along with the results of the present computations. Negligible Reynolds stress effects for viscous sublayer, which results in a linear profile, and logarithmic law of the wall for $(z^+ = z/\delta) > 30$ are recovered in the present computations which confirms the reasonable accuracy of the present work. Reynolds stress distribution across the channel, normalized by the wall-shear stress, was presented in Figure 5 along with the DNS data of Kim *et al.* [23]. It is observed that the computed Reynolds stress corresponds to the previously

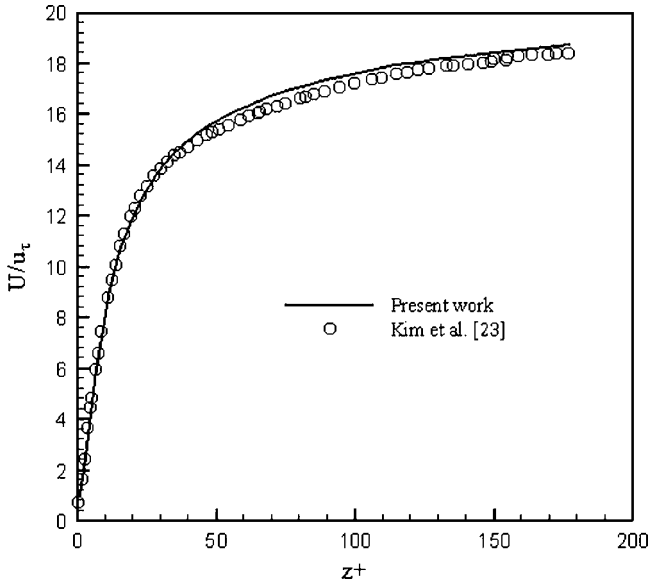

Figure 3. Comparison of mean velocity profile across the channel with DNS data.

DOI: 10.1002/fld

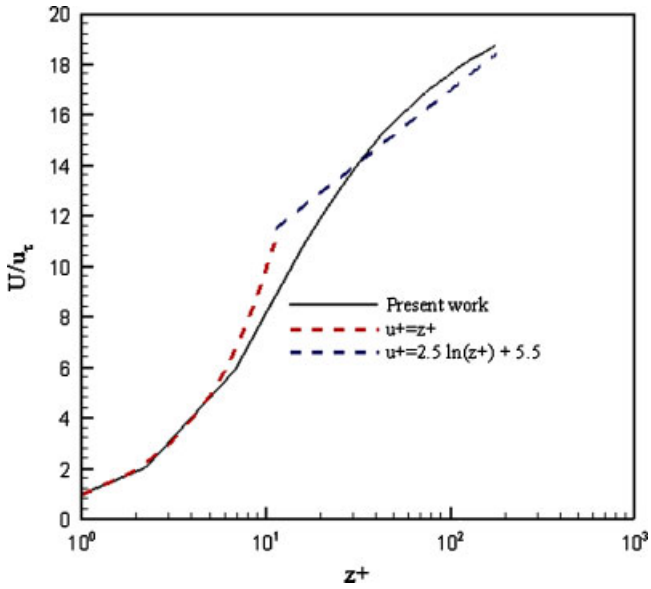

Figure 4. Comparison of mean velocity profile with the theoretical linear velocity profile in viscous sublayer and the logarithmic variations in the inertial sublayer.

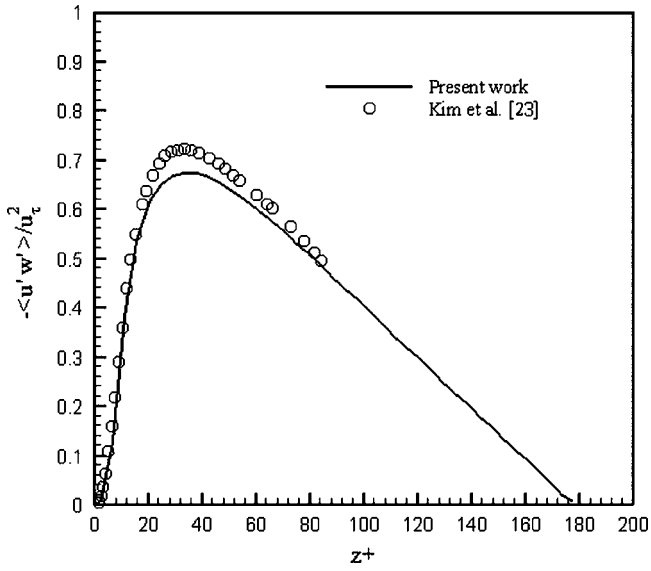

Figure 5. Distribution of Reynolds stress normalized by the wall shear stress across the channel.

computed DNS data with good accuracy for near wall region and far from the wall. The computed values follow the trend of DNS data with a small under-prediction for Z^+ (less than 7%) in the range between 15 and 70. Such behavior was observed in previous published works even with the more accurate dynamic SGS modeling of LES [21]; it seems that such small discrepancies are due to the less accurate LES as compared with DNS modeling of channel flow.

Figures 6–8 show variations of root mean-square (rms) of streamwise, spanwise and cross-stream velocity fluctuations respectively, along with the data from DNS based on Navier–Stokes equations [23] and those of GLBE with Smagorinsky model [19]. These statistics are important turbulent quantities which indicate the accuracy of turbulence model. As is observed in these figures, SISM with GLBE is capable of predicting turbulent fluctuations accurately. Figure 6 shows

DOI: 10.1002/fld

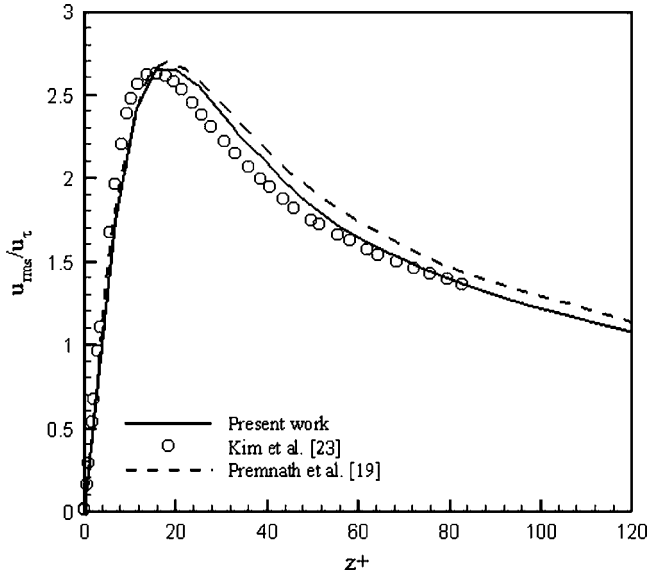

Figure 6. Distribution of root mean-square (rms) streamwise velocity fluctuations normalized by the wall shear velocity across the channel.

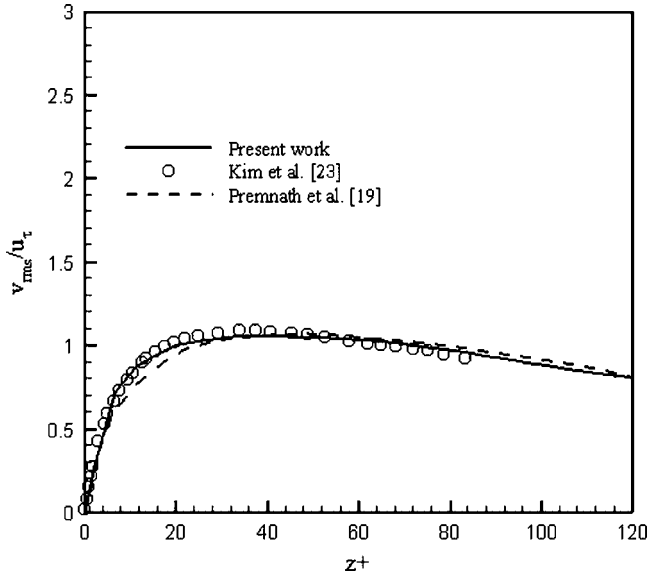

Figure 7. Distribution of root mean-square (rms) spanwise velocity fluctuations normalized by the wall shear velocity across the channel.

that SISM GLBE produces better results of rms velocity fluctuations as compared with GLBE with Smagorinsky model, when compared with DNS data.

Turbulence intensity profiles for different grid resolutions are shown in Figure 9. The width of the normalized grid filter, $\Delta^+ = \Delta/\delta$, is equal to 6 for $180 \times 90 \times 30$ and is equal to 4.5 for $240 \times 120 \times 40$. Although, in the first case a coarse resolution was used, the comparison between the results for different resolutions shows reasonable agreement. Besides, the present results confirm the stability of GLBE with SISM for $\Delta^+ = 6$. It was shown [11] that the required Δ^+ to ensure stable behavior with SRT model has previously been given as $\Delta^+ \leqslant 2.5$ for channel flow. The stability of

DOI: 10.1002/fld

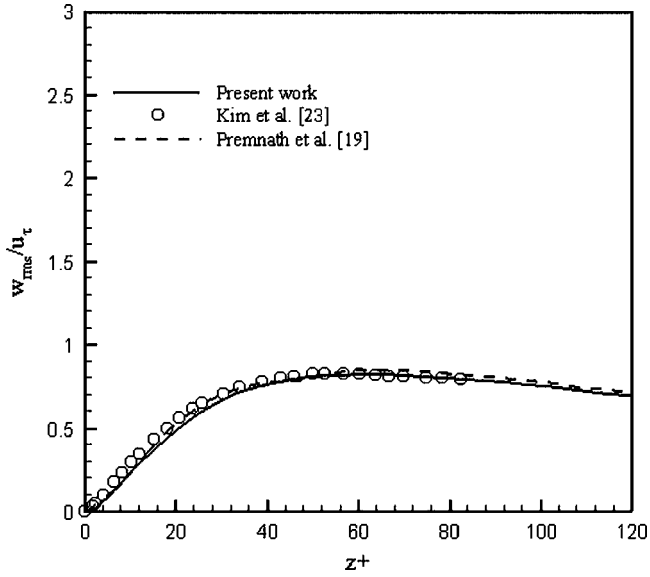

Figure 8. Distribution of root mean-square (rms) of wall-normal velocity fluctuations normalized by the wall shear velocity across the channel.

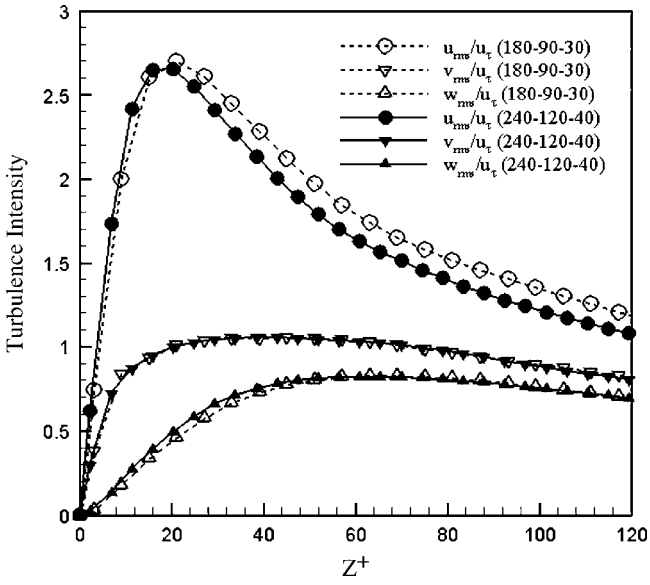

Figure 9. Turbulence intensity profiles for different grid resolutions.

GLBE with Smagorinsky model for $\Delta^+ = 6$ was shown in [19] and the present computations for this new framework confirm this subject.

A general view of instantaneous iso-vorticity surfaces of streamwise vorticity component is shown in Figure 10. These surfaces show vortical structures in cross-stream directions. It is well known that near-wall intensity of streamwise vorticity is larger than that of the channel center. Such behavior is clearly observed in Figure 10. A sample of instantaneous velocity fields in different planes is shown in Figure 11. Prediction of three-dimensional random patterns in turbulent channel flow shows the ability of the computational method in turbulent flow simulations. As illustrated in Figure 11(a), flow field in the $y-z$ plane shows a random pattern. Moreover, this figure shows the

DOI: 10.1002/fld

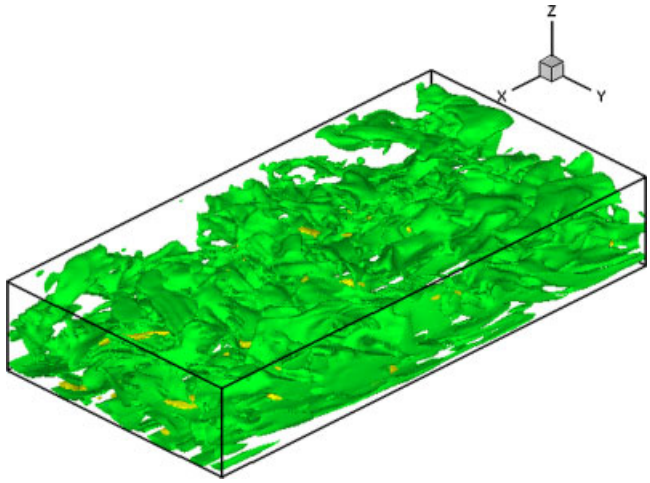

Figure 10. A snapshot of instantaneous iso-vorticity surfaces for streamwise vorticity component.

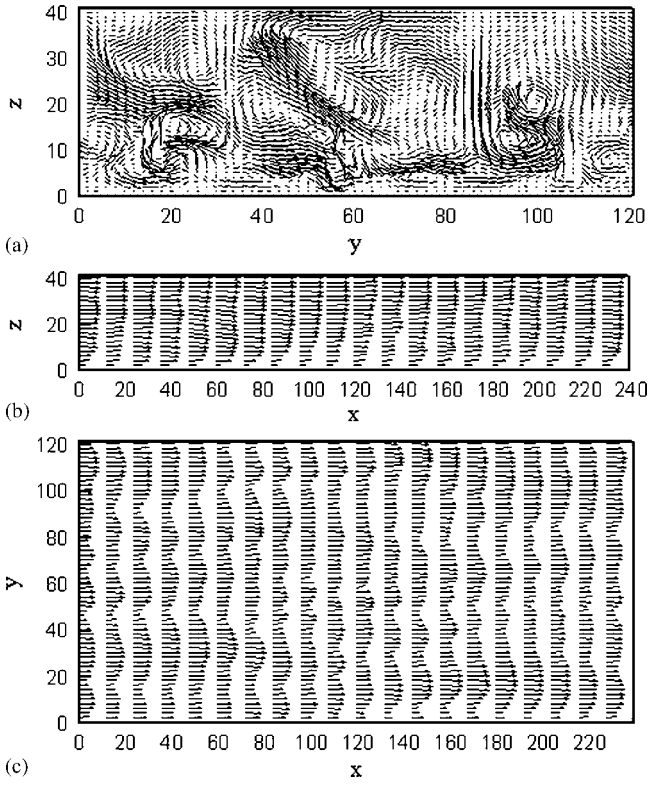

Figure 11. Sample instantaneous velocity vector plot in (a) $y-z$ plane; (b) $x-z$ plane; and (c) $x-y$ plane.

movement of near-wall eddies toward and away from the wall. Figure 11(b) displays the velocity vector plot in the $x-z$ plane. The random deviations from the expected profile are evidently shown. Velocity vectors at $y=H/5$ in the $x-y$ plane are displayed in Figure 11(c), which clearly shows the stream-wise velocity is predominant in this direction. Furthermore, the random pattern of flow field in this plane is visible.

DOI: 10.1002/fld

CONCLUSION

A Generalized Lattice Boltzmann Equation (GLBE) using multiple relaxation times along with a forcing term was employed for the simulation of turbulent channel flow at $Re_\tau = 180$. Turbulence simulation was done through LES with a recently proposed SGS model called shear-improved Smagorinsky model (SISM) [22]. This SGS model has shown reasonable results with a lower computational cost compared to turbulent flow simulation using CFD methods.

The results of turbulence statistics obtained from SISM LES were shown to be comparable to the Smagorinsky model with lower grid points employed in computations. Using SISM LES in GLBE reveals its ability to predict accurate results in computational framework of LBM.

Computational results for the mean turbulent quantities such as mean velocity distribution across the channel height, show good correspondence with DNS data. Comparison of the results for turbulence statistics such as rms velocity fluctuations with DNS and those obtained from Smagorinsky SGS model reveals the accuracy of the present computational results which are obtained using a smaller number of grid points. This computational framework predicts Reynolds stresses with a reasonable accuracy as compared to a high-resolution DNS data reported earlier. Various instantaneous velocity vectors and vorticity contours also showed complicated 3D vortical structures of turbulent channel flow. Based on the present computational results, it seems that GLBE with SISM-LES has the capability of predicting turbulent flow characteristics for turbulent wall flows with a relatively coarse grid as compared to DNS.

REFERENCES

1. Succi S. *The Lattice Boltzmann Equation for Fluid Dynamics and Beyond.* Oxford University Press: Oxford, 2001.
2. Chen S, Doolen G. Lattice Boltzmann method for fluid flows. *Annual Review of Fluid Mechanics* 1998; **30**:329–364.
3. Yu D, Mei R, Luo LS, Shyy W. Viscous flow computations with the method of Lattice Boltzmann equation. *Progress in Aerospace Science* 2003; **39**:329–367.
4. Aidun CK, Clausen JR. Lattice–Boltzmann method for complex flows. *Annual Review of Fluid Mechanics* 2010; **42**:439–472.
5. Qian YH, d'Humières D, Lallemand P. Lattice BGK models for Navier–Stokes equation. *European Physics Letters* 1992; **17**(6):479–484.
6. Djenidi L. Structure of a turbulent crossbar near-wake studied by means of Lattice Boltzmann simulation. *Physical Review E* 2008; **77**(3):036310–036312.
7. Djenidi L. Lattice–Boltzmann simulation of grid-generated turbulence. *Journal of Fluid Mechanic* 2006; **552**: 13–35.
8. Pope S. Ten questions concerning the large-eddy simulation of turbulent flows. *New Journal of Physics* 2004; **6**:35.
9. Ansumali S, Karlin I, Succi S. Kinetic theory of turbulence modeling: smallness parameter, scaling and microscopic derivation of Smagorinsky model. *Physica A* 2004; **338**:379–394.
10. Fernandino M, Beronov K, Ytrehus T. Large eddy simulation of turbulent open duct flow using a Lattice Boltzmann approach. *Mathematics and Computers in Simulation* 2009; **79**:1520–1526.
11. Lammers P, Beronov KN, Volkert R, Brenner G, Durst F. Lattice BGK direct numerical simulation of fully developed turbulence in incompressible plane channel flow. *Computers and Fluids* 2006; **35**(10):1137–1153.
12. Spasov M, Rempfer D, Mokhasi P. Simulation of a turbulent channel flow with an entropic Lattice Boltzmann method. *International Journal for Numerical Methods in Fluids* 2009; **60**:1241–1258.
13. Bhatnagar P, Gross EP, Krook MK. A model for collision processes in gases. I. Small amplitude processes in charged and neutral one component systems. *Physical Review* 1954; **94**(3):511–525.
14. Lallemand P, Luo LS. Theory of the Lattice Boltzmann method: dispersion, dissipation, isotropy, Galilean invariance, and stability. *Physical Review E* 2000; **61**(6):6546–6562.
15. d'Humières D, Ginzburg I, Krafczyk M, Lallemand P, Luo LS. Multiple-relaxation-time Lattice Boltzmann models in three dimensions. *Philosophical Transactions of the Royal Society A* 2002; **360**:437–452.
16. d'Humières D. Generalized Lattice Boltzmann equations. *Progress in Aeronautics and Astronautics* 1992; **159**: 450–458.
17. Krafczyk M, Tölke J, Luo LS. Large eddy simulation with a multiple-relaxation-time LBE model. *International Journal of Modern Physics B* 2003; **17**(1&2):33–39.
18. Yu H, Luo LS, Girimaji S. LES of turbulent square jet flow using an MRT Lattice Boltzmann model. *Computers and Fluids* 2006; **35**:957–965.

DOI: 10.1002/fld

19. Premnath KN, Pattison MJ, Banerjee S. Generalized Lattice Boltzmann equation with forcing term for computation of wall bounded turbulent flows. *Physical Review E* 2009; **79**(2):026703-1–026703-19.
20. Pattison MJ, Premnath KN, Banerjee S. Computation of turbulent flow and secondary motions in a square duct using a forced generalized Lattice Boltzmann equation. *Physical Review E* 2009; **79**(2):026704-1–026704-13.
21. Premnath KN, Pattison MJ, Banerjee S. Dynamic subgrid scale modeling of turbulent flows using Lattice–Boltzmann method. *Physica A* 2009; **388**:2640–2658.
22. Lèvêque E, Toschi F, Shao L, Bertoglio JP. Shear-improved Smagorinsky model for large-eddy simulation of wall-bounded turbulent flows. *Journal of Fluid Mechanics* 2007; **570**:491–502.
23. Kim J, Moin P, Moser R. Turbulence statistics in fully developed channel flow at low Reynolds number. *Journal of Fluid Mechanics* 1987; **177**:133–166.
24. Premnath KN, Abraham J. Three-dimensional multi-relaxation time (MRT) Lattice Boltzmann models for multiphase flow. *Journal of Computational Physics* 2007; **224**:539–559.
25. Chapman S, Cowling TG. *Mathematical Theory of Nonuniform Gases*. Cambridge University Press: New York, 1964.
26. Shao L, Sarkar S, Pantano C. On the relationship between the mean flow and subgrid stresses in large eddy simulation of turbulent shear flows. *Physics of Fluids* 1999; **11**(5):1229–1248.
27. Toschi F, Kobayashi H, Piomelli U, Iaccarino G. Backward-facing step calculations using the shear improved smagorinsky model. *Proceedings of the Summer Program 2006*, Center for Turbulence Research, Stanford University, Stanford, 2006.
28. Germano M, Piomelli U, Moin P, Cabot WH. A dynamic subgrid-scale eddy-viscosity model. *Physics of Fluids A* 1991; **3**:1760–1765.
29. Ladd AJC. Numerical simulations of particulate suspensions via a discretized Boltzmann equation. Part 1. Theoretical foundation. *Journal of Fluid Mechanics* 1994; **271**:285–309.

DOI: 10.1002/fld